Dual Cooperative Drive Circuit for Active Magnetic Bearings

Hsin-Lin Chiu, Nan-Chyuan Tsai*, Yi-Kai Chen
Department of Mechanical Engineering,
National Cheng Kung University,
70101, Tainan City, Taiwan.
*nortren@mail.ncku.edu.tw

***Abstract* – A Dual Cooperative Drive Circuit (DC^2) for Active Magnetic Bearing (AMB) units is proposed by this work. DC^2 operates in dual modes: Digital Driving Mode (DDM) and Analog Driving Mode (ADM). The proposed DC^2 manifests its superiorities in two aspects. (i). Compared to a traditional 2-level PWM (Pulse Width Modulation) drive circuit, the improvement degree of reducing the amplitudes of peak-to-peak current ripples is up to 74%. Reduction of ripples is specially beneficial for AMB units to retain the rotor at steady state, without significant reciprocated fluctuation repeatedly. (ii). DC^2 provides high current slew rate so that the response of AMB is fast and quick enough to regulate the rotor back to the desired position within a very short time period. These two advantages by DC^2 are fairly pertinent to the problems of rotor position regulation. The proposed DC^2 exhibits its satisfactory performance either in computer simulations or realistic experiments.**

Keywords-drive circuit; power amplifier; direct current; pulse width modulation; active magnetic bearing

I. Introduction

Analog drive circuits [1-2] possess the merits of high linearity and low Electromagnetic Interference (EMI). However, the energy efficiency of analog drive circuits is inherently poor because a great percentage of the energy power will be converted into heat at the corresponding driver Integrated Circuits (ICs). By contrast, the power loss is limited for the digital drive circuits [3-4]. Nevertheless, the current spike problem caused by digital drive circuits is more serious than that by analog drive circuits.

Due to analog drive circuits and digital drive circuits having their own irreplaceable advantages, a Dual Cooperative Drive Circuit (DC^2) for AMB units is proposed by this paper. The proposed DC^2 can conduct under two distinct operation modes: Digital Driving Mode (DDM) and Analog Driving Mode (ADM). Taking the advantage of the complementary characteristics of interchange between DDM and ADM, the proposed DC^2 exhibits both high current slew rate and relatively mild current ripples.

II. Design of Dual Cooperative Drive Circuit (DC^2)

As well known, MOSFET (Metal-Oxide-Semiconductor Field-Effect Transistor) and IGBT (Insulated Gate Bipolar Transistor) are of low on-state resistance, low gate charge, high-power requirement and low price. Therefore, they are widely employed in vehicles, communication devices, and energy industries. Roughly speaking, owing to the on-off frequency of MOSFETs is higher than that of IGBTs, MOSFETs are more often adopted for the drive circuits applied to Active Magnetic Bearings (AMBs) whose purpose is to regulate the radial position deviation of rotors, particularly at high speed.

A. Output Characteristics of N-channel Enhancement MOSFETs

The applied MOSFET to DC^2 is an n-channel enhancement transistor whose output characteristics are shown in Fig. 1 [5], where i_D is the drain current, V_{GS} the gate-source voltage, V_{DS} the drain-source voltage, and V_t the gate threshold voltage. As long as the MOSFET operates in its saturation region, the MOSFET is, to some extent, analogous to a voltage-controlled linear power amplifier.

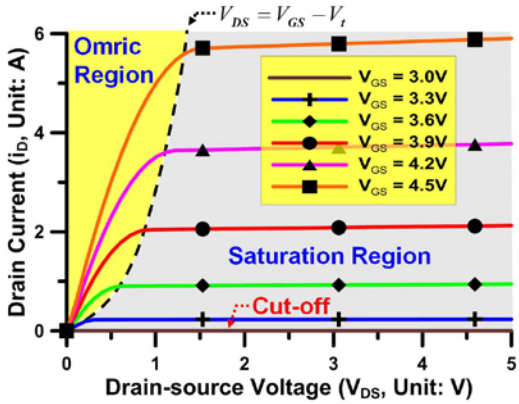

Figure 1. Output characteristics of n-channel enhancement MOSFET [5].

B. DC^2 for AMBs

The configuration of the proposed Dual Cooperative Drive Circuit (DC^2) for AMBs is shown in Fig. 2. In fact, the main concept of DC^2 is initiated by the semi-passive H-bridge drive circuit [6]. Compared with the H-bridge drive circuit, merely two essential electronic components, i.e., a Digital-to-Analog Converter (DAC) and an Analog Multiplexer (Analog MUX) are additionally included by DC^2. The real-time coil current is transduced and converted into voltage signal by a Current Sensor (CS) and then

ISBN 978-80-261-0722-4, © University of West Bohemia, 2018

this voltage signal is fed to the LPF (Low-Pass Filter) to reduce or suppress the current ripple embedded in the feedback signal.

Basically, DC^2 operates in dual modes: Digital Driving Mode (DDM) and Analog Driving Mode (ADM). Under DDM, the supplied DC voltage to MOSFETs is high so that AMBs can adjust the levitation force promptly against the external disturbance to the rotor, with no need of conversion cycle of digital commands to analogous currents. That is, DDM is suitable to be applied for the ***transient state*** of the rotor/AMB dynamics. On the other hand, as the rotor/AMB dynamics is at ***steady state***, instead, ADM takes over to provide a relatively stable levitation force to the rotor, with a relatively mild ripple effect to cause the rotor wobble.

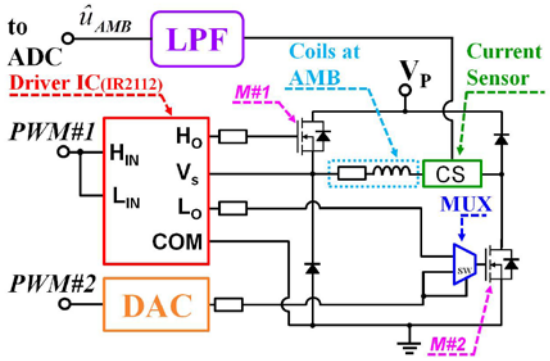

Figure 2. Circuit configuration of DC^2.

1) Digital Drive Mode (DDM)

From the viewpoint of signal processing, the corresponding circuit under DDM is nothing but a switching power amplifier. The operation states of the switching power amplifier are illustrated in Fig. 3. Under DDM, solely one PWM signal, i.e., ***PWM#1***, is required to switch on/off the two MOSFETs, marked as ***M#1*** and ***M#2*** in Fig. 3, simultaneously. When the two MOSFETs are turned on, shown in Fig. 3(a), the switching power amplifier operates at ***charge state***. When the two MOSFETs are both turned off, shown in Fig. 3(b), the power amplifier is at ***discharge state***.

2) Analog Drive Mode (ADM)

The corresponding operation states under ADM are depicted in Fig. 4. Under ADM, two commands, namely, ***PWM#1*** and ***PWM#2*** shown in Fig. 2, are required to control the two MOSFETs, ***M#1*** and ***M#2***, respectively. ***PWM#1*** is applied to adjust the drain-source voltage of ***M#2***, while ***PWM#2*** is utilized to regulate the AMB coil current. Under ADM, ***M#2*** always operates within saturation region so that its characteristics can be analogous to a voltage-controlled power transducer. It is noted that any MOSFET which operates within the saturation region has to satisfy the constraint: $V_{DS} > V_{GS} - V_t$. However, the higher across voltage, V_{DS}, over a MOSFET, the more energy consumed by this MOSFET. That is, a trade-off or real-time adjustment strategy is required to be included. As a result, ***M#1*** is applied to regulate the drain-source voltage of ***M#2***, V_{DS}, to minimize, to some extents, the energy consumption by ***M#2***. Besides, the drain current over ***M#2***, which is identical to the current applied at AMB coil, is slightly dependent of V_{DS} over ***M#2***.

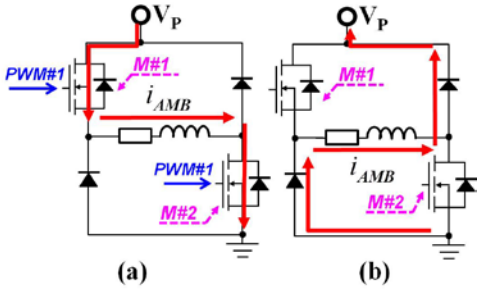

Figure 3. Operation states of DC^2 under DDM: (a) charge state; (b) discharge state.

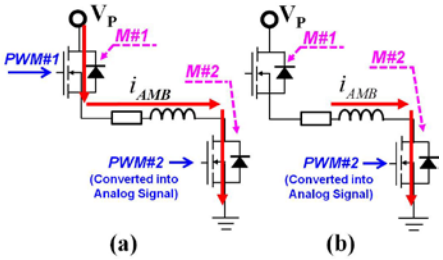

Figure 4. Operation states of DC^2 under ADM: (a) charge state; (b) discharge state.

III. Pulse Width Modulation-Tuning Processors (PWM-TPs)

For DC^2 conducts under two distinct operation modes, i.e., DDM and ADM, two Pulse Width Modulation-Tuning Processors (PWM-TPs) are required to appropriately tune the output current to the AMB units. Besides, a switch along with a ***Schmitt trigger***, hereafter named as "**mode selector**" in this paper, is applied to determine the timing of change between these two modes, i.e., DDM and ADM. The schematic diagram for the PWM-TPs of DC^2 is shown in Fig. 5. i_{AMB}^{ref} is the desired current applied to the AMB coils while u_{AMB}^{ref} is the corresponding voltage command. The constant resistance with respect to u_{AMB}^{ref} over i_{AMB}^{ref}, i.e., R_{iu} in Fig. 5, is set as 1 Ω. On the other hand, i_{AMB} is the actual current at the AMB coils, and $\hat{u}_{AMB}$ is the converted voltage with respect to the measured current by the equipped Current Sensor (CS) upon i_{AMB}. The constant resistance for i_{AMB} converted to $\hat{u}_{AMB}$ is set as 1 Ω. If the error between u_{AMB}^{ref} and $\hat{u}_{AMB}$ is significant, DC^2 operates under DDM so that the output current by DC^2, $\hat{u}_{AMB}$, can quickly catch up the desired quantity, u_{AMB}^{ref}. On the contrary, once the output current gets close to the desired quantity, DC^2 operates under ADM to generate a relatively stable current.

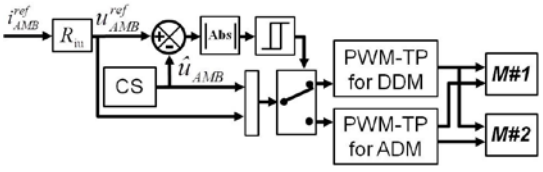

Figure 5. Schematic diagram for two PWM-TPs within DC^2.

A. PWM-TP for DDM

One of the merits of DC^2 under DDM is: relatively high current slew rate of supplied output current. In other words, DDM is suitable to be employed to the ***transient state*** of rotor/AMB dynamics. Under DDM, merely one digital control sequence, i.e., ***PWM#1***, is required to turn ***M#1*** and ***M#2*** on/off. For there always exists high-frequency current ripples under DDM, the derivative action of a PID controller would certainly downgrade the quality of output current. Therefore, a PI controller, shown in Fig. 6, is employed to tune the duty ratio of ***PWM#1***.

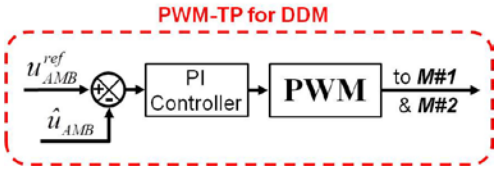

Figure 6. Schematic diagram for PWM-TP under DDM.

B. PWM-TP for ADM

Owing to one of the shortcomings of DDM: inevitable fluctuation of the supplied voltage downgrades the quality of the output current to AMB coils, another operation mode, i.e., ADM, is joined to provide a relatively stable output current to regulate the ***steady state*** of rotor position. Under ADM, ***M#2*** operates, within saturation region, to work like a voltage-controlled power transistor. As long as the MOSFET operates within its saturation region, the variation of output current is strongly dependent of the gate-source voltage, V_{GS}. Consequently, the digital control sequence to adjust the output current of DC^2, i.e., ***PWM#2***, is converted into analog fashion with a Digital-to-Analog Converter (DAC) *prior to* feeding to ***M#2***. It is noted that as a MOSFET operates within its saturation region, the higher the voltage over the MOSFET, the more energy consumed by the MOSFET. Therefore, ***PWM#1*** is employed to tune the drain-source voltage of ***M#2*** as DC^2 operates under ADM. The schematic diagram for PWM-TP under ADM is depicted in Fig. 7. A Low Pass Filter (LPF) is employed to reduce the amplitudes of current ripples lurked in the feedback signal. Afterwards, the error between u_{AMB}^{ref} and $\hat{u}_{AMB}$ is fed to a PI controller to tune the desired output current precisely. In addition, this error is also applied for fine-tuning the duty ratio of ***PWM#1*** such that the energy consumption can be reduced. Furthermore, there are two compensators, i.e., K_b^V and K_b^I shown in Fig. 7, are included to adjust the duty ratios of ***PWM#1*** and ***PWM#2*** respectively.

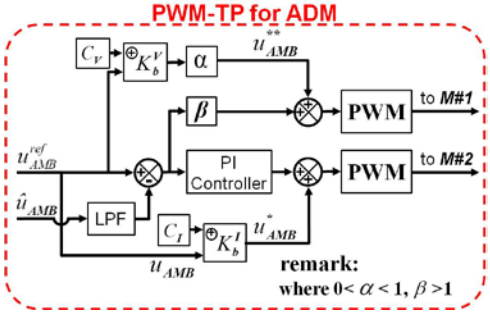

Figure 7. Schematic diagram for PWM-TP under ADM.

IV. Computer Simulations

In this section, the computer simulations for PWM-TPs to track the desired output are undertaken to verify the capability of DC^2. It is assumed that the reference signal is to track a step-wise function. The desired voltage to drive the AMB coil, V_P, is set as 40 VDC. The thresholds of "***Switched On***" and "***Switched Off***" points of the employed ***Schmitt trigger*** are set as $0.05A$ and $0.01A$ respectively. As long as the error between i_{AMB} and i_{AMB}^{ref} is over $0.05A$, then DC^2 is controlled by PWM-TP under DDM. On the contrary, as the error between i_{AMB} and i_{AMB}^{ref} is less than $0.01A$, then DC^2 is controlled by PWM-TP under ADM.

A. Simulation Results under DDM Solely

The operation of DC^2 under DDM is analogous to a 2-level PWM drive circuit. Its reference is nothing but a sequence of step-wise signal whose value is all limited by [0, 1.5A]. The time duration of each step is set as $5\,ms$. The step-wise reference and the corresponding tracking error of output current under DDM are shown in Fig. 8. It can be observed that the amplitudes of steady state errors are all below $10\,mA$ under DDM. However, the peak-to-peak amplitudes of current ripples are about $30\,mA$. Since the current ripples are too large such that the regulation performance of AMB upon the position deviation of rotor is much downgraded, the other operation mode, namely ADM, has to be included to reduce the aforesaid current ripples.

B. Simulation Results by DC^2

For DDM and ADM possess their own particular merits, DDM and ADM are combined to constitute the proposed DC^2. The tracking error by DC^2 is shown in Fig. 9. It can be observed that the tracking errors by DC^2 are all below $\pm 1\,mA$ owing to the well cooperation of DDM and ADM. The comparisons of tracking errors under DDM and DC^2 are summarized in Table I. Compared with DDM, the improvement of reducing peak-to-peak amplitude of current ripples by DC^2 is up to 94% as i_{AMB} is by $0.01A$ under steady-state circumstance. On the other hand, as i_{AMB} is by $1.5A$ under transient-state circumstance, the improvement degree of reducing the peak-to-peak amplitude of current ripples by DC^2 is about 74%. The comparison, in terms of the peak-to-peak amplitude of current ripples, between DDM and DC^2 is concluded by Table II. As i_{AMB} is within [0, 1.5A], the maximum values of tracking errors under DDM and DC^2 are about $9.36mA$ and $0.90mA$ respectively. To be more evidently compared, as i_{AMB} is $0.01A$, the tracking error by DC^2 is under 3.6% while the tracking error by DDM is up to 93.6%. As i_{AMB} is much greater than $0.01A$, the tracking error by DC^2 is reduced to 0.3% or below.

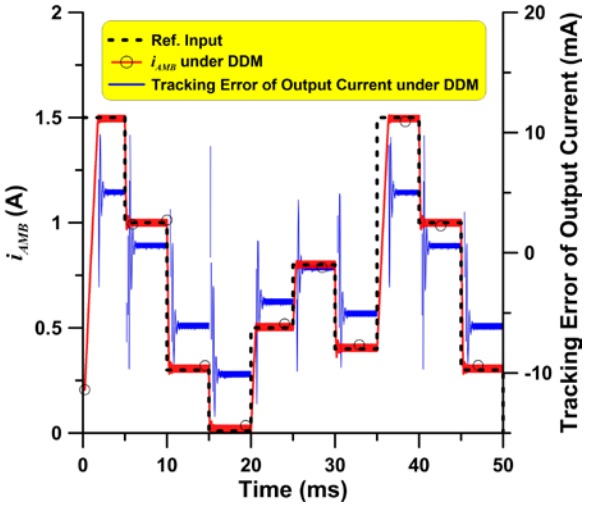

Figure 8. Tracking error of output current under DDM.

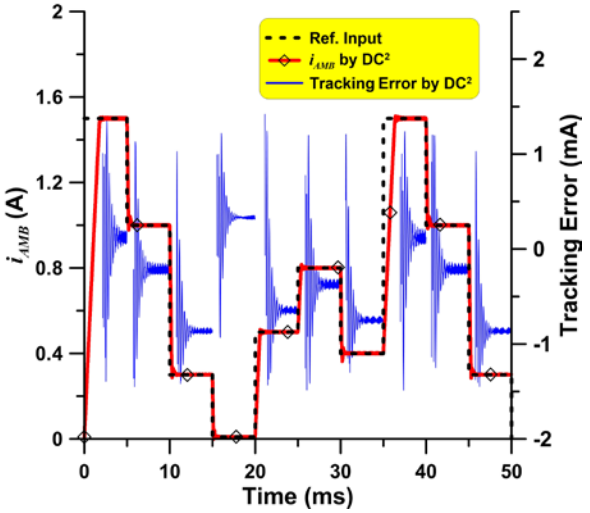

Figure 9. Tracking error of output current under DC^2.

TABLE I. TRACKING ERROR OF i_{AMB}

A: Amplitude of i_{AMB} (A)	DDM		DC^2	
	B: TE (mA)	C: Error C=B/A (%)	D: TE (mA)	E: Error E=D/A (%)
0.01	9.36	93.60	0.36	3.600
0.3	6.36	2.120	0.90	0.300
0.4	5.32	1.330	0.79	0.198
0.5	4.33	0.866	0.69	0.138
0.8	1.47	0.184	0.42	0.053
1	0.86	0.086	0.27	0.027
1.5	5.25	0.350	0.19	0.013

Note: TE is the abbreviation of "Tracking Error".

TABLE II. PEAK-TO-PEAK AMPLITUDES OF CURRENT RIPPLES

Amplitude of i_{AMB} (A)	DDM	DC^2	
	A: PPACR (mA)	B: PPACR (mA)	C: Imp. C=(A-B)/A
0.01	31.4	1.7	94.59%
0.3	30.5	3.4	88.85%
0.4	30.2	3.7	87.75%
0.5	30.0	4.2	86.00%
0.8	29.3	5.2	82.25%
1	28.9	5.8	79.93%
1.5	27.7	7.2	74.01%

Note: PPACR is the abbreviation of "Peak-to-Peak Amplitude of Current Ripple"

V. CONCLUSIONS

A novel circuit design of power amplifier applied for Active Magnetic Bearings (AMBs), named as Dual Cooperative Drive Circuit (DC^2), is proposed in this study. DC^2 can conduct under two operation modes: Digital Driving Mode (DDM) and Analog Driving Mode (ADM). As the rotor/AMB dynamics is at the ***transient state***, the DC^2 operates under DDM to provide quick actuation to AMBs by higher current slew rate. On the other hand, as the rotor/AMB dynamics is at ***steady state***, DC^2 operates under ADM to provide an output current with relatively mild current ripples so that the ***steady state*** can be well retained, without significant reciprocated fluctuation. Besides, all the signals fed to DC^2 are of Pulse Width Modulation (PWM) fashion. Consequently, DC^2 can be directly driven by a Digital Signal Processing (DSP) chip. Compared to a traditional 2-level PWM drive circuit, the improvement degree of reducing the amplitudes of peak-to-peak current ripples is up to 74 % by DC^2. On the other hand, the improvement degree of reducing the tracking error of output current is up to 68.6% by DC^2. The total power losses by MOSFETs and diodes are 0.31W and 0.53W under DDM and cooperative mode respectively. Though the power loss under cooperative mode is slightly higher than that under DDM, by taking advantages of cooperation between DDM and ADM, the proposed DC^2 manifests the superiorities of both high current slew rate and small current ripples.

ACKNOWLEDGMENT

This research was partially supported by Ministry of Science and Technology (Taiwan) with 3-years Grant MOST 105-2221-E-006-070-MY3. The authors would like to express their appreciations.

REFERENCES

[1] S. Carabelli, F. Maddaleno, and M. Muzzarelli, "High-efficiency linear power amplifier for active magnetic bearings," IEEE Trans. Ind. Elec., vol. 47, pp. 17–24, January 2000.

[2] G. Gong, H. Ertl, and J. W. Kolar, "Novel tracking power supply for linear power amplifiers," IEEE Trans. Ind. Elec., vol. 55, pp. 684–698, January 2008.

[3] H. Zhang, J. Fang, and H. Liu, "Online current signal de-noising of magnetic bearing switching power amplifier based on lifting wavelet transform," IET Elec. Power App., vol. 10, pp. 799–806, May 2016.

[4] Y. Ren, and J. Fang, "Current-sensing resistor design to include current derivative in PWM H-bridge unipolar switching power amplifiers for magnetic bearings," IEEE Trans. Ind. Elec., vol. 59, pp. 4590–4600, December 2012.

[5] K. S. Oh, "AN9010 MOSFET Basics," ON Semiconductor, July 2000.

[6] G. Schweitzer, and E. H. Maslen, "Magnetic Bearings: Theory, Design, and Application to Rotating Machinery," Springer Science & Business Media, 2009.